PROGRESS IN THE DEVELOPMENT OF A GRAZING-INCIDENCE INSERTION DEVICE X-RAY BEAM POSITION MONITOR*

B.X. Yang[†], G. Decker, S. H. Lee, P. Den Hartog, and K. W. Schlax,
Advanced Photon Source, Argonne National Laboratory, Argonne, IL 60439, USA

Abstract

Recently, a grazing-incidence insertion device x-ray beam position monitor (GRID-XBPM) was proposed that would withstand the intense x-ray beam power of the future APS undulators [1]. In this design, the functions of a front-end limiting aperture and a high-heat load XBPM are combined. Beam position is determined by the hard x-ray fluorescence footprint on the aperture/XBPM. This design minimizes the impact of soft x-ray background radiation and improves XBPM accuracy, especially at lower undulator power/larger gap settings. In this work, we report on the design progress of a GRID-XBPM for a beamline with two in-line Undulator A's with a total power of 18 kW. Computer simulation of its performance and engineering design details are presented.

INTRODUCTION

The Advanced Photon Source facility is planning a major upgrade that would include improvement in x-ray beam stability. The stability goals are listed in Table 1 [2] and are to be achieved on beamlines with as much as 21 kW. Located far from the undulator source, the XBPMs have been useful in monitoring beam pointing angles. However, the widely used, photo-emission-based XBPMs presently installed in the APS are sensitive to soft radiation generated by the bend magnets and corrector magnets upstream and downstream of the undulator sources. The steering of the e-beam through the undulator moves these background beams on the XBPM even when the undulator beam is center at the XBPM. The movements create false readings and reduce effectiveness of carefully designed background subtraction algorithms [3], especially when the undulator is at larger gap and emits lower power. We are developing a grazing-incidence insertion-device XBPM (GRID-XBPM) that derives x-ray beam position from the fluorescence x-ray (XRF) footprint on the limiting apertures of the beamline. By combining the two optical components of the beamline, we eliminated any problem of their possible misalignment with respect to each other, thus allowing a reduction of the aperture size and transmitted x-ray power on user optics downstream. In addition to these advantages, since the GRID-XBPM can be implemented to measure center-of-mass of the x-ray fluorescence footprint when pinhole-camera-like optics are used for position readout [1], it offers a solution for long-standing XBPM design issues for elliptical undulators, which have a donut-shaped power distribution. Our recent progress in simulation and engineering designs of this XBPM is described here.

*Work supported by the U.S. Department of Energy, Office of Science, Office of Basic Energy Sciences, under contract number DE-AC02-06CH11357.

[†]bxyang@aps.anl.gov

Table 1: APS Beam Stability Goals (rms)

		Position	Angle
Horizontal:	AC (0.1-200 Hz)	3 μm	0.53 μrad
	long-term (one-week)	5 μm	1.0 μrad
Vertical:	AC (0.1-200 Hz)	0.42 μm	0.22 μrad
	long-term (one-week)	1.0 μm	0.5 μrad

THE FIRST XBPM

Table 2 lists the XBPM accuracy goals translated from Table 1, where we took 70% of the total allowed x-ray beam motion at 20 m as the minimum accuracy needed. Figure 1 shows the layout of an undulator line and front end with the GRID-XBPM. Due to the "Decker distortion" [3] used for all undulators, two corrector-bend magnets are next to the undulator straight sections, generating a background radiation pattern that is fixed relative to the undulator beam axis. Figure 2 shows the measured distribution of the magnetic field of the correctors [4], scaled to give a total deflection of 1 mrad. We observe that the peak field is well below the main dipole (0.6 T) and the fringe field is even weaker. Within 0.1 mrad of the undulator axis, the magnetic field is less than 0.05 T and the nominal critical energy is below 1.8 keV. Since this energy is well below the Cu *K*-edge of 9 keV, they have negligible impact on the XRF background signal, as validated in experiments [1].

Table 2: APS GRID-XBPM Accuracy Goals (rms)

	Horizontal	Vertical
AC (0.1-200 Hz)	7 μm	3 μm
Long-term (one-week)	14 μm	10 μm

Undulator White-Beam Power Pattern

In designing an efficient GRID-XBPM we would like to use a limiting aperture as small as acceptable to the x-ray beam users. We will use an aperture of 4 mm (H) × 1.5 mm (V) at 20 mm from the source as our model for the current design studies. Figure 3 shows the two-dimensional patterns of the x-ray beam power at the XBPM location. From maximum to minimum gaps, the patterns show a smooth, single peak. In the horizontal plane, the width of the power profile may be estimated with a Gaussian fit, with its rms width given by, approximately,

Copyright © 2011 by PAC'11 OC/IEEE — cc Creative Commons Attribution 3.0 (CC BY 3.0)

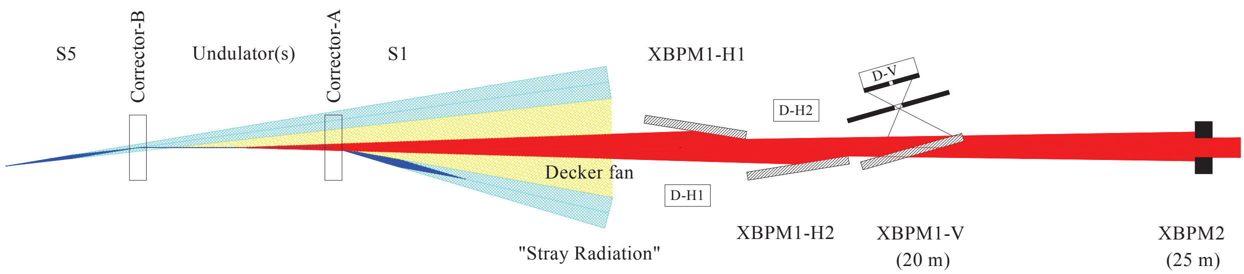

Figure 1: Top view of the undulator and XBPM showing the main design idea of GRID-XBPM and XBPM2.

$$W_x = \frac{aS}{\gamma}\left(K^3 + b^3\right)^{1/3}, \qquad (1)$$

where the aperture distance S = 20 m and the fit parameters a = 1.67 and b = 0.46 (see Fig. 4). Figure 5 shows the power profile in the vertical plane at minimum gap (K = 2.76), along with the monochromatic beam profiles near the first harmonic photon energy. Two substantial wings exist outside of the aperture.

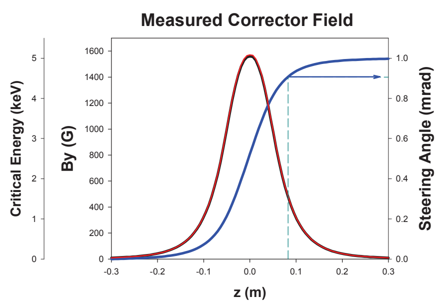

Figure 2: Black curve shows the measured magnetic field B_y of the correct magnet at the entrance and exit of an APS insertion device. Red curve shows the nominal bend magnet critical energy for the field value. Blue curve shows the cumulative steering angle up to the location.

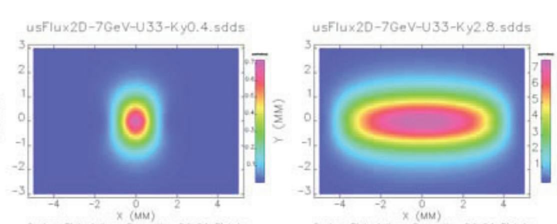

Figure 3: X-ray power pattern for Undulator A for K = 0.4 and 2.8, respectively.

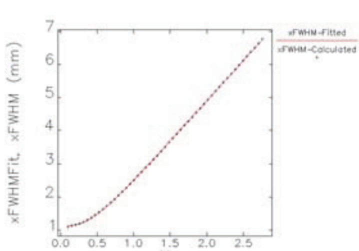

Figure 4: Horizontal width of the Undulator A power profile as a function of deflection parameter K.

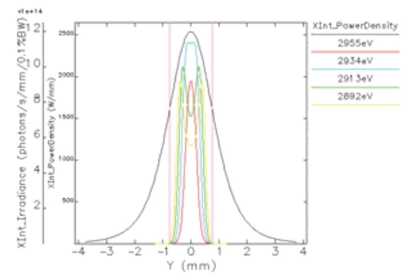

Figure 5: Vertical power profile and monochromatic beam profiles at and near the first harmonic of Undulator A (K = 2.76). Two red vertical lines denote the vertical aperture.

X-ray Fluorescence Pattern

Unlike the power distributions, the x-ray fluorescence intensity distributions show more shape variations for different K values. We calculated the intensity distribution using grazing incidence geometry, which allows more high-energy photons to be absorbed near the surface and contributes to XRF signals. Figure 6 shows the XRF intensity distributions at maximum gap (K = 0.4) and minimum gap (K = 2.8). In these cases, the first and the third harmonic energies are just above the Cu K-edge, respectively. Compared with the power maps, the XRF distributions are more "square-ish." However, between K = 1.1 and 1.8, the second harmonic is the dominant contributor to the K-edge excitation, and the XRF intensity map resembles a dumbbell.

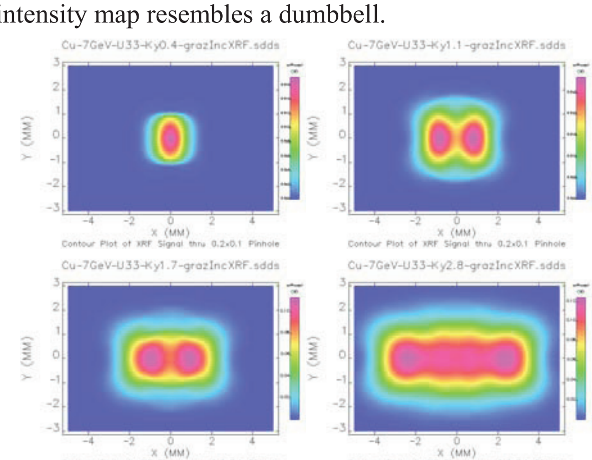

Figure 6: XRF intensity from a Cu target in grazing incidence for Undulator A; K = 0.4 (upper left), 1.1 (upper right), 1.7 (lower left), and 2.8 (lower right).

Copyright © 2011 by PAC'11 OC/IEEE — cc Creative Commons Attribution 3.0 (CC BY 3.0)

For $K < 1.0$, significant XRF intensity exists only above and below the 4 mm × 1.5 mm aperture. For $K > 1.5$, strong XRF intensity comes from the horizontal borders, while the XRF distributions on the center 4 mm of the upper and lower border do not give good information on the centroid of the beam.

THE SECOND XBPM

Projection of the undulator beam through the first XBPM's 4 mm × 1.5 mm aperture gives us a 5 mm × 1.9 mm x-ray beam cross section at 25 m from the source. We plan to implement a four-quadrant photoemission (TEY = total electron yield) detector, clipping 1-mm x-ray beam from each side of the beam on the left and right, resulting in a 3 mm × 2 mm pass-through aperture, which agrees with a popular choice of APS users. Since the first XBPM has a small aperture, its combination with the downstream quad-detector forms a pinhole camera with a 4:1 demagnification: for x-ray beam centered on the XBPM1, an upward displacement of the source causes the x-ray beam to shift down at 25 m.

In Figure 7, we show the calculated TEY intensity from a Au target. Since only the surface layer contributes to the TEY, grazing incidence will only increase the TEY signal current without changing the intensity distribution pattern. Here we assume that the small aperture of the XBPM1 blocks most background radiation and improves the S/N of the "pinhole camera." This assumption needs to be tested in further simulations and experiments.

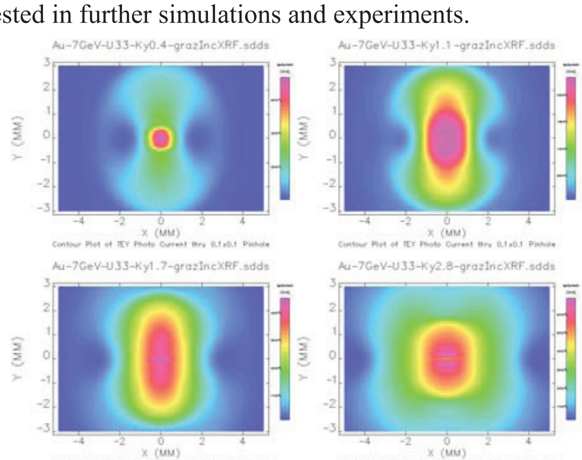

Figure 7: TEY intensity from a gold target in grazing incidence for Undulator A; K = 0.4 (upper left), 1.1 (upper right), 1.7 (lower left), and 2.8 (lower right).

ENGINEERING DESIGN

Engineering design of the first, GRID-XBPM is at an advanced stage. Figure 8 shows its 3D engineering model: A granite table provides a sturdy support for the entire assembly. A 5-axis cam-mover system provides a motion range of ±1 mm and ±0.75 mm in horizontal and vertical planes, respectively. On the table top, a fixed mask matches the XBPM acceptance aperture with the upstream collimator; two independent vertical plates, XBPM-H1 and XBPM-H2, accept the beam ±2 mm away from the beam axis; and a pair of vertical slits, XBPM1-V, intercepts the beam ±0.75 mm above and below the beam axis. While the two vertical plates are equipped with XRF intensity detectors, the two BPM1-V slits are equipped with a pinhole-camera-like optics with a quadrant detector readout. The quad detector is responsible for reading the vertical beam position at all gap settings and horizontal position at wide gaps ($K < 1.0$). The two intensity detectors for the vertical plates are used to provide horizontal beam position at narrower gaps ($K > 1.0$). The smooth transition between these horizontal detectors is highly desirable, and will be a subject of experimental studies.

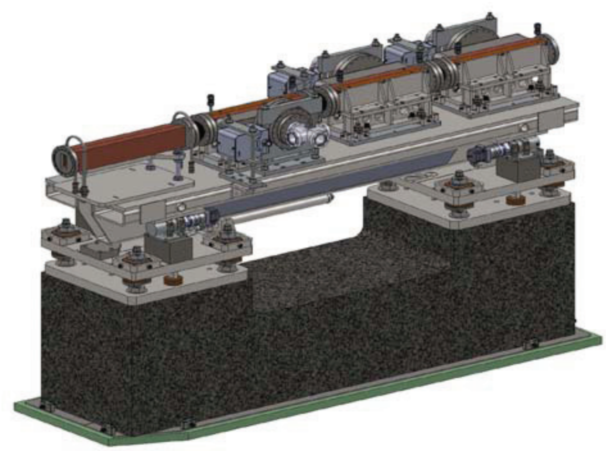

Figure 8: 3D model of the GRID-XBPM design: From left to right on the table top: fixed mask, XBPM-H1, XBPM-H2, and XBPM-V.

SUMMARY

We calculated undulator x-ray power and XRF intensity distribution to support the design of GRID-XBPM. We further proposed a second XBPM in the spirit of x-ray pinhole cameras for measurements of the source position. Further modeling will be needed to derive suitable expressions to disentangle contributions of the beam position and pointing angle changes in the two XBPM readings. The progress of the engineering design is on schedule for an experimental test of the first article within a year.

We would like to thank Roger Dejus and Hairong Shang for their help in undulator calculations, Mohan Ramanathan and Ali Khounsary for helpful discussions on XBPM designs and testing.

REFERENCES

[1] B. X. Yang, G. Decker, S. H. Lee, and P. Den Hartog, Beam Instrumentation Workshop, Santa Fe, p. 233, (2010).
[2] G. Decker, Beam Instrumentation Workshop, Santa Fe, p. 74, (2010).
[3] Phys. Rev. Spec. Top., Accel. Beams 2(11), (1999) 112801.
[4] C. Doose, private communications on magnetic field measurements.

Copyright © 2011 by PAC'11 OC/IEEE — cc Creative Commons Attribution 3.0 (CC BY 3.0)